Information Theory and Applications (ITA 2019): San Diego, February 11-15, 2019

SAN- Slotted Aloha-NOMA a MAC Protocol for M2M Communications

Asim Mazin, Mohamed Elkourdi, and Richard D. Gitlin, *Life Fellow, IEEE*
Innovation in Wireless Information Networking Lab (*i*WINLAB)
Department of Electrical Engineering, University of South Florida, Tampa, Florida 33620, USA
Email:{ asimmazin,elkourdi}@mail.usf.edu, richgitlin@usf.edu

***Abstract*—This paper describes Slotted Aloha-NOMA (SAN), a novel medium access control (MAC) protocol, directed to Machine to Machine (M2M) communication applications in the 5G Internet of Things (IoT) networks. SAN is matched to the low-complexity implementation and sporadic traffic requirements of M2M applications. Substantial throughput gains are achieved by enhancing Slotted Aloha with non-orthogonal multiple access (NOMA) and a Successive Interference Cancellation (SIC) receiver that can simultaneously detect multiple transmitted signals using power domain multiplexing. The gateway SAN receiver adaptively learns the number of active devices using a form of multi-hypothesis testing and a novel procedure enables the transmitters to independently select distinct power levels. Simulation results show that the throughput of SAN exceeds that of conventional Slotted Aloha by 0.8 packet/sec and that of CSMA/CA by 0.2 packet/sec with a probability of transmission of 0.03, with a slightly increased average delay owing to the novel power level selection mechanism. Multiple-input-multiple-output beamforming (2x2 MIMO BF) further increases the data throughput to 1.31 packet/sec compared with 0.36 packet/sec in conventional Slotted Aloha with 3 optimum power levels and reduces the average channel access delay of the SAN protocol from 0.13 sec to 0.09 sec.**

***Index Terms*—Slotted-Aloha, M2M communication, multiple hypothesis testing, NOMA, CSMA/CA, IoT.**

I. Introduction

The rapid growth of both the number of connected devices and the data volume that is expected to be associated with the IoT applications, has increased the popularity of Machine-to-Machine (M2M) type communication within 5G wireless communication systems [1]. Uncoordinated random access schemes have attracted lots of attention in the standards of cellular network as a possible method for making massive number of M2M communication possible with a low signaling overhead [2], [3].

The MAC protocols for wireless networks have been intensively investigated in the existing literature and can be classified into three main categories as contention-based, contention-free, and hybrid protocols that incorporate the advantages of contention-based and contention-free protocols.

In the contention-based protocols, the nodes in the M2M scenario contend to access the shared medium. Although the contention-based MAC protocols match the M2M requirements in terms of having cost-efficient implementation, they are unsuited to the dense M2M deployment due to frequent collisions, which results in low throughput. Pure-Aloha, Slotted Aloha, and Carrier-Sense Multiple Access with Collision Avoidance CSMA/CA are examples of such contention-based MAC protocols [4]. ZigBee is among those technologies and one of the most commonly used standards in IoT. The MAC protocol in ZigBee is IEEE 802.15.4 [5] and uses CSMA/CA.

Contention-free protocols (scheduled-based) pre-assign the resources to the devices in the network. Based on the assigned resources, there are three well known scheduled based TDMA, FDMA, and CDMA, and hybrids such as OFDMA which combines TDMA and FDMA, where orthogonal signals are assigned to the devices in the network. In the context of M2M communications, the static channel allocation results in poor utilization at low loads (where the number of active devices is small) [4]. Dynamic contention-free protocols that assign the resources adaptively based on the active devices in the network are better suited for M2M in terms of resource utilization; however, the dynamic allocation of the resources demands extra overhead.

Hybrid MAC protocols are designed to combine the advantages of the contention-free and the scheduled-based MAC protocols. In [6] CSMA is used during the contention period (CP) and TDMA is used during the transmission period (TP). The successful devices during the contention period are guaranteed time slots during the transmission period. In [7] the performance of a framed hybrid MAC protocol was formulated as an optimization problem to determine the trade-off between CP and TP lengths that increase the total system throughput in M2M communications. The high rate of collisions during the reservation stage is the bottleneck that prevents hybrid protocols from achieving high utilization in dense M2M networks.

The recently proposed Slotted Aloha-NOMA (SAN) protocol [8] exploits the simplicity of slotted Aloha (used during the CP) and the superior throughput of non-orthogonal multiple access (NOMA) (used during the TP) and its ability to resolve collisions via use of a successive interference cancellation (SIC) receiver [9], [10]. SAN, which is an extension of the Aloha-NOMA protocol [11], is a promising candidate MAC protocol that can be utilized for low complexity IoT devices. In [12] NOMA is applied to multichannel Slotted Aloha to enhance the throughput with respect to conventional multichannel slotted Aloha without the need for any bandwidth expansion. The SAN protocol is a promising method for not requiring scheduling, apart from frame synchronization, in which all IoT devices transmit to the gateway at the same

time on the same frequency band and has high throughput as will be demonstrated in this paper.

In this paper, we present the following features of the SAN protocol: the receiver adaptively learns the number of active devices (which is not known a priori) using a form of multi-hypothesis testing, a comparison of SAN with CSMA/CA and Slotted Aloha in terms of throughput and average delay, and the enhancement, in terms of throughput and access delay from multiple-input multiple-output beamforming (BF-SAN) [13]. Simulation results are performed to show that the SAN protocol performs significantly better than Slotted Aloha and CSMA/CA in the low probability regime of transmission in terms of throughput.

This paper is organized as follows. Section II discusses the SAN protocol architecture and operation, Section III presents simulation results that compare the success probability (throughput) and the average delay of both protocols, and the papers conclusion is in Section V.

II. Slotted Aloha-Noma Protocol

A. Slotted Aloha-NOMA overview

NOMA has emerged as a promising technology in 5G networks for many applications, and the SAN protocol is a synergistic combination of the low complexity Slotted Aloha protocol with the high throughput feature of NOMA. The main bottleneck of Slotted Aloha systems is the low throughput caused by the high number of collisions, which can be addressed by NOMA. In SAN the signaling overhead is reduced in the detection phase of the proposed protocol where the number of active IoT devices are detected by the gateway using a form of multiple hypotheses testing, which is further explained in Section II-B. It is also an energy efficient protocol due to the fact that a SIC receiver resolves collisions, and thus minimizes retransmission. The SAN protocol can be suitable for various scenarios where many IoT devices are transmitting simultaneously on the same frequency with different power levels to an IoT gateway, and then the received signals can be separated via the use of a SIC receiver. A sample illustration of this scenario is depicted in Fig. 1 as a smart home with an IoT network. In this model, IoT devices send their data to the IoT gateway at the beginning of the slot using the SAN protocol and the IoT gateway distinguish the signals with a SIC receiver.

The SAN scheme increases the throughput significantly beyond that of conventional slotted Aloha due to the use of multiple power levels, which are considered additional channels in the power domain (and matched to the SIC receiver levels).

The SAN and BF-SAN protocol flowchart is depicted in Fig.2. First, the IoT gateway transmits a beacon signal to announce its readiness to receive packets. Next, the IoT devices with packets ready to transmit send a training sequence to aid the gateway in detecting the number of active IoT devices in the medium. The IoT gateway detects the number of devices requesting transmission via a form of multiple hypotheses testing, as further explained in Section II-B, and

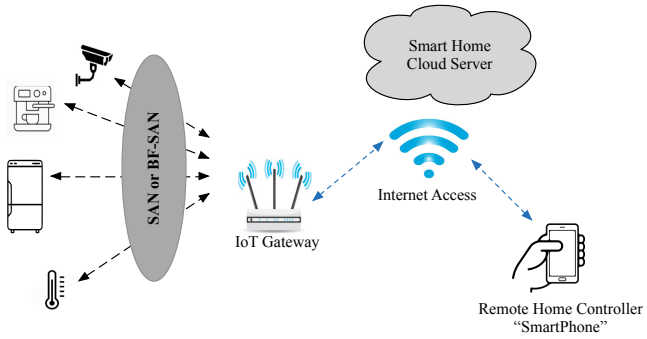

Fig. 1. A use case of SAN or BF-SAN in the smart home with IoT.

adjusts the degree of SIC receiver for the optimum power levels. In practice, the SIC receiver has a fixed range of optimum power levels (e.g., m= 2, 3). If the IoT devices are registered with the gateway instead of using multi-hypothesis testing, implementation would be simpler; however, this will significantly increase the length of the control phase and thus decrease the payload or throughput considering the potentially large number of IoT devices. Third, if the detected number of active IoT devices is not in the range of the SIC capability, the IoT gateway aborts the transmission and starts the frame again by sending a new beacon signal and implying that the active transmitters use a random backoff. If the detected number of devices is in range, the IoT gateway broadcast the degree of SIC to the transmitters, and then each active IoT device randomly picks one of receiving antennas using a pre-calculated precoding matrix (in the case of BF-SAN protocol) and also picks one of the optimum power levels. If the choices are distinct (at each receiving antenna in BF-SAN), the SIC receiver can decode the self-identifying signals (device ID + payload) and then the gateway sends an ACK. However, if the active IoT devices did not select distinct power levels, the reselection process is repeated, and after a few attempts k if there is no successful transmission, the users receive a NACK and enter a random back-off mode, which will improve fairness among the users and will allow for the possibility of fewer active users in the next session (which will improve the probability of successful transmission). It should be clear, that the SAN and BF-SAN protocols will be most efficient when there are a small number of active devices, so that the probability of using the optimum power levels, after one or two random tries, is high.

B. Multiple Hypothesis Testing

The detection of active devices starts after the IoT devices send their transmission request to IoT gateway as illustrated in Fig. 2. After receiving the beacon, all the IoT devices send at the same power level a training sequence of length L using the slotted Aloha protocol. The superimposed received signal at the IoT gateway from N active transmitting IoT devices is given by

$$\mathbf{y} = \mathbf{H}\mathbf{s} + \mathbf{w}, \tag{1}$$

where $\mathbf{H} = [h_1, , h_2, ..., h_N] \in \mathbb{R}^{1\times N}$, h_n is the channel gain between the n^{th} IoT device and the IoT gateway, $\mathbf{s} \in \mathbb{R}^{N\times L}$ is the transmit sequence (e.g. BPSK) from N IoT active devices and $\mathbf{w} \in \mathbb{R}^{1\times L}$ is the additive white Gaussian noise with zero mean and variance σ^2. The multiple hypothesis test is used to detect the number of N active IoT devices from the total M IoT devices. The following hypotheses testing procedure is used to sequentially detect the number of active devices.

$$\begin{aligned}
&\mathcal{H}_0 : \text{Received signal contains only noise} \\
&\quad \mathbf{y} = \mathbf{w}, \\
&\mathcal{H}_1 : \text{Received signal contains} \\
&\quad \text{data from at least one IoT device} \\
&\quad \mathbf{y} = h_1 s_1 + \mathbf{w}, \\
&\mathcal{H}_N : \text{Received signal contains} \\
&\quad \text{data from at most } N \text{ IoT devices} \\
&\quad \mathbf{y} = \mathbf{H}\mathbf{s} + \mathbf{w}
\end{aligned} \tag{2}$$

We assume $h_n = 1$, $\forall n \in \{1, 2, ..., N\}$. Following the Neyman-Pearson (NP) test, we can write the Likelihood Ratio (LR) testing [14] $\mathcal{H}_N$ Vs. $\mathcal{H}_{(N-1)}$ as in (3), where $\mathbf{s}_n \in \mathbb{R}^{1\times L}$ is the transmitted sequence from n^{th} IoT device. By taking the logarithm, (3) is simplified to (4).

The NP detector or the test statistics in (4) compares the sample mean of the received signal to the threshold $\gamma\prime$ to decide on a hypothesis $\mathcal{H}_N$ or $\mathcal{H}_{N-1}$. The NP test terminates if the number of detecting devices exceeds the SIC receiver optimum power levels, which are 3 levels in this paper. To compute the threshold $\gamma\prime$ in (4) for a desired probability of false alarm P_{FA}, which occurs when deciding $\mathcal{H}_N$ if the test in (4) is greater than the threshold $\gamma\prime$, so that P_{FA} can be written as

$$P_{PF} = p(T(\mathbf{y}) > \gamma\prime). \tag{5}$$

Since the test in (4) under both hypotheses is a Gaussian distribution, that $T(\mathbf{y}) \sim \mathcal{N}(\sum_{l=0}^{L-1}\sum_{n=1}^{N-1}\mathbf{s}_n, \frac{\sigma^2}{L})$ under $\mathcal{H}_{N-1}$ and $T(\mathbf{y}) \sim \mathcal{N}(\sum_{l=0}^{L-1}\sum_{n=1}^{N}\mathbf{s}_n, \frac{\sigma^2}{L})$ under $\mathcal{H}_N$, we rewrite (5) as

$$P_{FA} = Q\left(\frac{\gamma\prime - \sum_{l=0}^{L-1}\sum_{n=1}^{N}\mathbf{s}_n}{\sqrt{\frac{\sigma^2}{L}}}\right) \tag{6}$$

Thus the threshold $\gamma\prime$ is given by

$$\gamma\prime = Q^{-1}(P_{FA})\sqrt{\frac{\sigma^2}{L}} + \sum_{l=0}^{L-1}\sum_{n=1}^{N-1}\mathbf{s}_n \tag{7}$$

Following the same steps, the probability of detecting the number of active devices is

$$P_D = Q\left(\frac{\gamma\prime - \sum_{l=0}^{L-1}\sum_{n=1}^{N-1}\mathbf{s}_n}{\sqrt{\frac{\sigma^2}{L}}}\right) \tag{8}$$

From (7) and (8) the probability of detection P_D can be written as a function of signal to noise ratio SNR

$$P_D = Q\left(Q^{-1}(P_{FA}) + \frac{\sum_{l=0}^{L-1}\sum_{n=1}^{N}\mathbf{s}_n - \sum_{l=0}^{L-1}\sum_{n=1}^{N-1}\mathbf{s}_n}{\sqrt{\frac{\sigma^2}{L}}}\right). \tag{9}$$

The receiver operating characteristic (ROC) curve of the energy detector is shown in Fig.3 and probability of correct detection of the number of active users as a function of the SNR for $P_D = 0.1$ is shown in Fig.4. Observe that the detection performance increases monotonically and smoothly with increasing SNR.

III. Simulation Results

In this section, the simulation results are presented to evaluate the performance of SAN and BF-SAN protocols based on throughput, and average delay compare to Slotted Aloha and CSMA/CA. Throughout the simulation, we assume there is one IoT gateway with N_t transmitting antenna and a total of *M* IoT devices. A binomial distribution is considered to model the random number of active IoT devices *N*, each with probability of transmission p_T.

$$P_T(N; p_T, M) = \binom{M}{N} p_T^N (1 - p_T)^{M-N} \tag{10}$$

Fig. 5 shows the throughput of SAN for different values of p_T, *M*=50 and *k*=3 attempts for the random selection of distinct optimum power levels (so, the probability of success should be 0.4). The throughput is the average number of successful transmissions for each probability of transmission over time. As expected, we observe that the throughput decreases with increasing probability of transmission in both protocols. More importantly, we can see that the throughput of the SAN protocol is weighted by the average payload of successful transmissions and always higher than that of the slotted Aloha protocol. When the probability of transmission is 0.03, the throughput of SAN with 3 power levels performs better than the CSMA/CA and has 5 times higher throughput than that of (conventional) slotted Aloha. This demonstrates that NOMA with a SIC receiver can help improve the throughput of slotted Aloha. However, the throughput of SAN becomes lower than CSMA/CA for a probability of transmission greater than 0.06 (i.e. increase of offered load from the IoT devices), which is not surprising since for *M* = 50 the average number of active devices exceeds the number of acceptable power levels (SIC capability). The improved performance of CSMA/CA in a higher probability of transmission regime is due to the collision avoidance mechanism. It can be noted from Fig. 7. that adding more power levels (6 power levels) to SAN increase the throughput at the expense of the average delay, which is discussed next.

The second performance metric is the average delay as shown in Fig. 10. In the simulation, the average delay is composed of propagation delay, data processing delay, random backoff delay, sensing delay (in CSMA/CA) and selecting unique power levels attempts (in SAN and BF-SAN). Observe

$$\frac{p(\mathbf{y};\sum_{n=1}^{N}\mathbf{s}_n,\mathcal{H}_N)}{p(\mathbf{y};\sum_{n=1}^{N-1}\mathbf{s}_n,\mathcal{H}_{N-1})}=\frac{exp[-\frac{1}{\sigma^2}(\mathbf{y}-\sum_{n=1}^{N}h_n\mathbf{s}_n)^T(\mathbf{y}-\sum_{n=1}^{N}h_n\mathbf{s}_n)]}{exp[-\frac{1}{\sigma^2}(\mathbf{y}-\sum_{n=1}^{N-1}h_n\mathbf{s}_n)^T(\mathbf{y}-\sum_{n=1}^{N-1}h_n\mathbf{s}_n)]}\lessgtr_{\mathcal{H}_{N-1}}^{\mathcal{H}_N}\gamma, N=1,...M. \tag{3}$$

$$T(\mathbf{y})=\frac{1}{L}\sum_{l=0}^{L-1}\mathbf{y}\lessgtr_{\mathcal{H}_N}^{\mathcal{H}_{N-1}}\frac{2\sigma^2\ln\gamma-((\sum_{n=1}^{N-1}h_n\mathbf{s}_n)^T(\sum_{n=1}^{N-1}h_n\mathbf{s}_n)+(\sum_{n=1}^{N}h_n\mathbf{s}_n)^T(\sum_{n=1}^{N}h_n\mathbf{s}_n))}{-2(\sum_{n=1}^{N-1}h_n\mathbf{s}_n+\sum_{n=1}^{N-1}h_n\mathbf{s}_n)}=\gamma\prime. \tag{4}$$

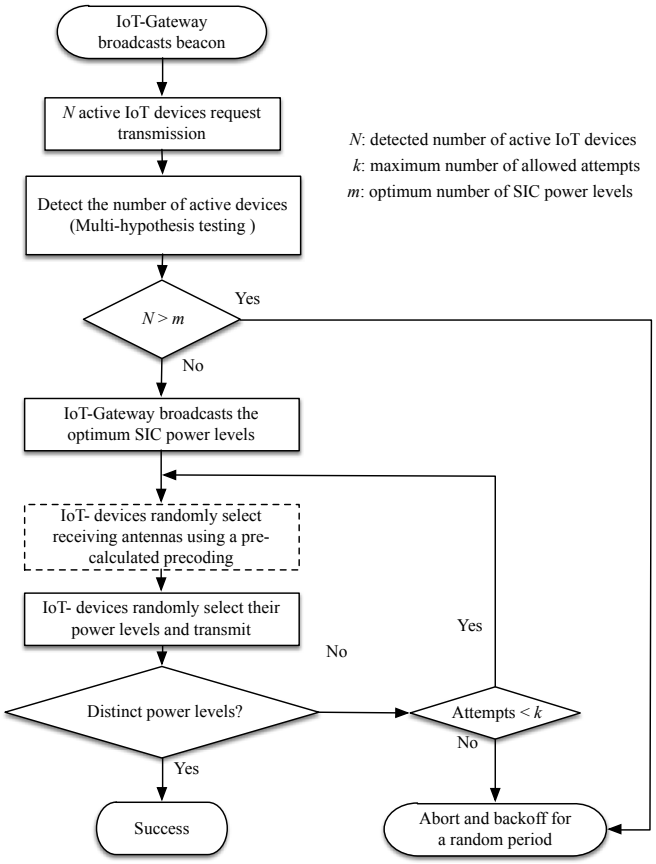

Fig. 2. SAN and BF-SAN (box with dashed line) protocol.

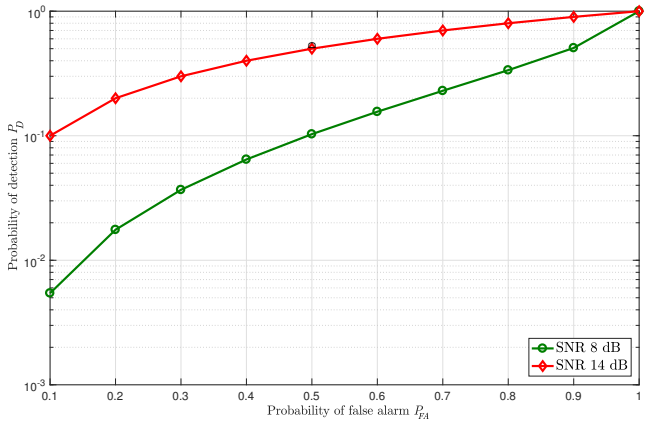

Fig. 3. ROC of the energy detector.

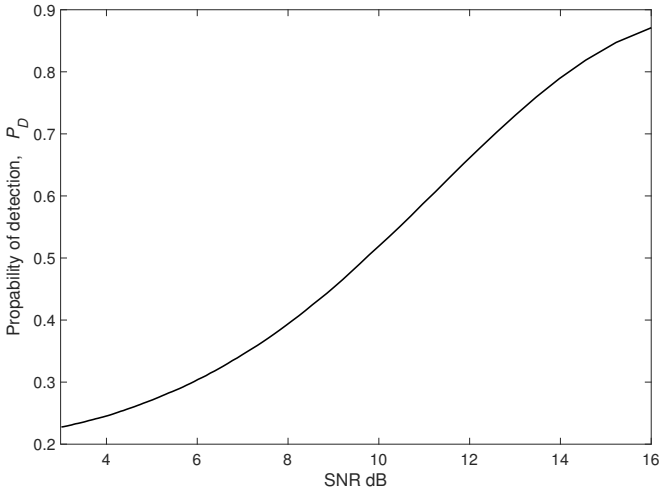

Fig. 4. Detection probability of the number of active devices as a function of SNR.

that the average delay of SAN is larger than the CSMA/CA in the low probability of transmission due to the unique power levels selection process, which enables the higher throughput as mentioned above. The more attempts allowed for picking the distinct optimum power levels, the higher the throughput that can be achieved at the cost of increased delay. Since the backlogged IoT devices (i.e., failed to transmit in the previous try) have not been considered to rejoin the transmission queue, the average delay reported at a higher probability of transmission is the propagation delay and the random backoff delay.

Fig. 7 shows the throughput of BF-SAN when $M = 100$, $m = 3$ optimum power levels, k=3 attempts, $N_t = 2$, $N_r = 2$ and for different values of p_T. In the simulation, the throughput is defined as the number of successful transmissions for each probability of transmission. As expected, we can observe that the throughput decreases as the probability of transmission increases. More importantly, we can see that the throughput of the BF-SAN protocol is always higher than that of SAN and conventional Slotted Aloha protocols. In particular, when the probability of transmission is 0.15, the throughput of BF-SAN is almost 60 times higher than that of conventional slotted Aloha and 2 times higher than SAN. This demonstrates that BF-SAN provides a dramatic improvement in throughput in comparison with conventional Slotted Aloha and SAN protocol due to the additional "virtual" sub-channels in space and power domains.

In Fig. 8 and Fig. 9 we show the throughput and channel access delay performance of BF-SAN and SAN when $k = 2, 3$

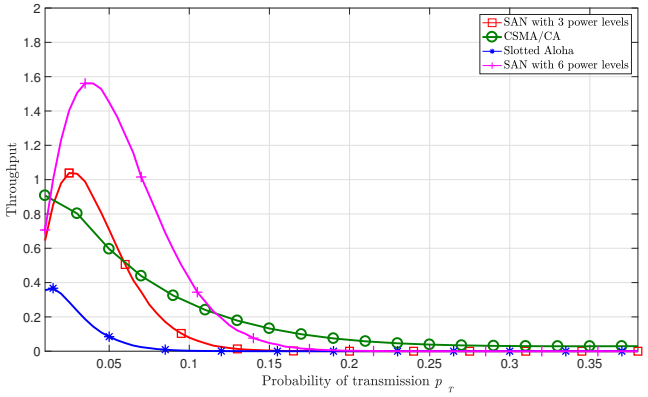

Fig. 5. The throughput of SAN vs. Slotted Aloha and CSMA/CA for different values of probability of transmission M=50.

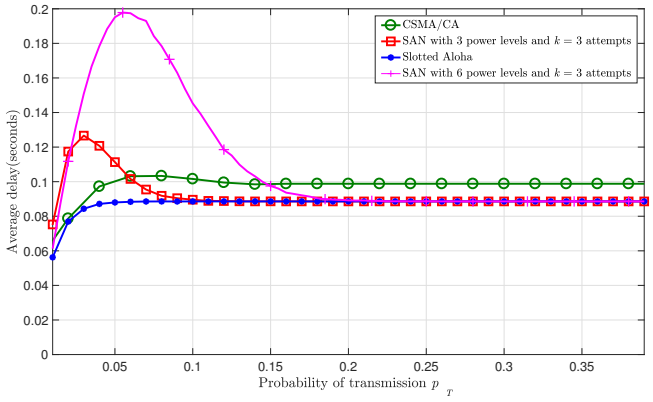

Fig. 6. The average delay of SAN, Slotted Aloha and CSMA/CA.

attempts, $M = 100$, $m = 3$, $N_t = N_r = 2$ and for different values of probability of transmissionp_T. It is shown that BF-SAN when $k = 2$ can still achieve a higher throughput that SAN when $k = 3$ with a lower channel access delay resulting from the attempts for picking distinct power levels.

In order to see the impact of the number of optimum power levels on the throughput of BF-SAN, we show the throughput of BF-SAN for different power levels in Fig. 10. For $M = 100$, $k = 2, 3, 5$ and probability of transmission of 0.05, the throughput of SAN increases with the increase in optimum power levels (SIC degree). For example, SAN with 3 power levels has a higher throughput than SAN with 2 power levels. However, the throughput improvement becomes insufficient for optimum power levels greater than 5 (saturation in the throughput gain). Also, the simulation results in Fig. 8, shows the impact of the number of attempts, for picking distinct optimum power levels, on throughput for different optimal power levels. The more attempts allowed for picking the optimum power levels, the higher the throughput that can be achieved at the cost of increased delay.

IV. Conclusion

This paper describes the advantages of the Slotted Aloha-NOMA (SAN) protocol and its beam-forming enhanced version BF-SAN for M2M communications in IoT networks. These random access protocols are easy to implement, and compatible with the limited-power and low complexity requirements of IoT devices. The synergistic combination of Slotted Aloha, NOMA, and SIC receivers was demonstrated to significantly improve the throughput performance with respect to the conventional Slotted Aloha and CSMA/CA protocols at a low probability of transmission. BF-SAN reduces the SAN channel access delay, which results from the attempts for picking distinct power levels. Simulation results have shown that BF-SAN can achieve higher throughput than SAN with a smaller number of attempts and consequently a lower channel access delay. SAN and its enhanced BF-SAN protocol can be quite important for massive M2M communication in IoT networks. Future research directions are to investigate the fairness of both MAC protocols and study the effect of the backlogged IoT devices that rejoin the transmission queue.

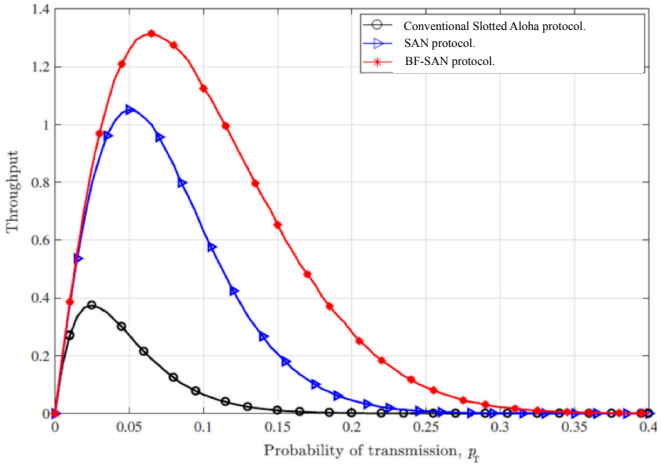

Fig. 7. The throughput of BF-SAN vs. SAN and conventional Slotted Aloha protocols when $M = 100$, $m = 3$, $k = 3$, and for different values of probability of transmission. M=50.

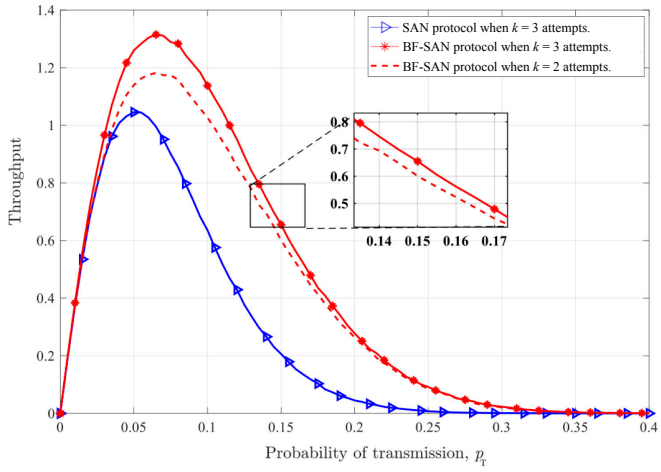

Fig. 8. The throughput of BF-SAN vs. SAN for different values of probability of transmission when $M = 10$ $m = 3$, and $k = 2, 3$ attempts.

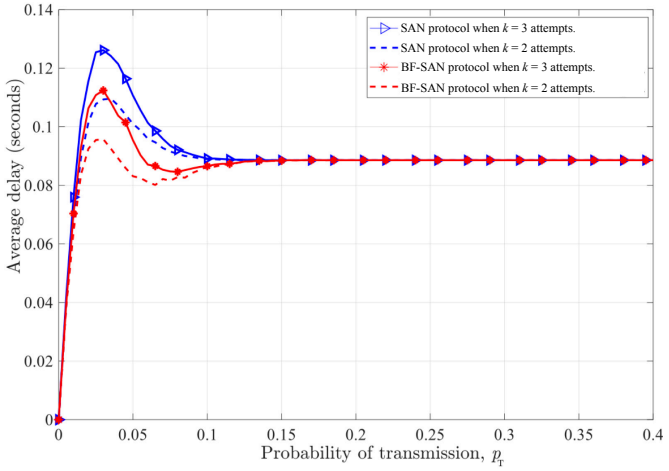

Fig. 9. The throughput of BF-SAN vs. SAN for different values of probability of transmission when $M = 10$ $m = 3$, and $k = 2, 3$ attempts.

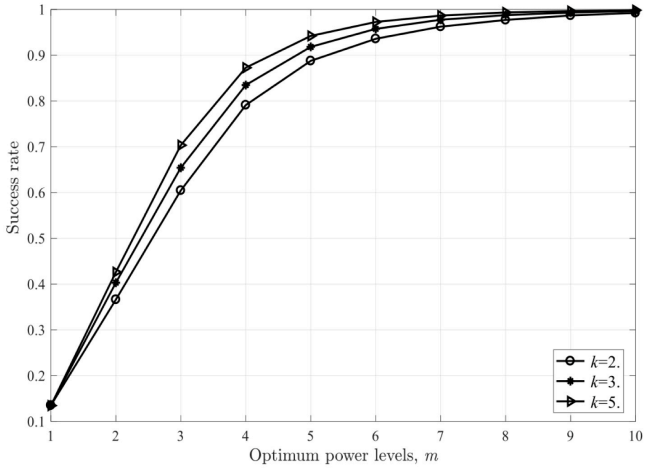

Fig. 10. The success rate of BF-SAN for different values of optimum power levels when $M = 100$, and $k = 2, 3, 5$ attempts.

REFERENCES

[1] M. N. Tehrani, M. Uysal, and H. Yanikomeroglu, "Device-to-device communication in 5G cellular networks: challenges, solutions, and future directions," *IEEE Communications Magazine*, vol. 52, no. 5, pp. 86–92, May 2014.

[2] 3GPP, "Study on RAN improvements for machine-type communications," TS 37.868 V11.0, October 2011.

[3] 3GPP, "Evolved universal terrestrial radio access (E-UTRA); medium access control (MAC) protocol specification," TS 36.321 V13.2.0, October 2016.

[4] D. Agrawal and Q. Zeng, *Introduction to Wireless and Mobile Systems*. Cengage Learning: Boston, MA, USA, 2016.

[5] "IEEE Standard for Low-Rate Wireless Networks," *IEEE Std 802.15.4-2015 (Revision of IEEE Std 802.15.4-2011)*, pp. 1–709, April 2016.

[6] Y. Liu, C. Yuen, J. Chen, and X. Cao, "A scalable hybrid mac protocol for massive m2m networks," in *2013 IEEE Wireless Communications and Networking Conference (WCNC)*, April 2013, pp. 250–255.

[7] W. Saad, S. A. El-Feshawy, M. Shokair, and M. I. Dessouky, "Optimised approach based on hybrid MAC protocol for M2M networks," *IET Networks*, vol. 7, no. 6, pp. 393–397, 2018.

[8] M. Elkourdi, A. Mazin, E. Balevi, and R. D. Gitlin, "Enabling slotted Aloha-NOMA for massive M2M communication in IoT networks," in *2018 IEEE 19th Wireless and Microwave Technology Conference (WAMICON)*, April 2018, pp. 1–4.

[9] Y. Saito, Y. Kishiyama, A. Benjebbour, T. Nakamura, A. Li, and K. Higuchi, "Non-orthogonal multiple access (NOMA) for cellular future radio access," in *2013 IEEE 77th Vehicular Technology Conference (VTC Spring)*, June 2013, pp. 1–5.

[10] X. Wang and H. V. Poor, "Iterative (Turbo) soft interference cancellation and decoding for coded CDMA," *IEEE Transactions on Communications*, vol. 47, no. 7, pp. 1046–1061, Jul 1999.

[11] E. Balevi, F. T. A. Rabee, and R. D. Gitlin, "Aloha-NOMA for massive machine-to-machine IoT communication," in *2018 IEEE International Conference on Communications (ICC)*, May 2018, pp. 1–5.

[12] J. Choi, "NOMA-based random access with multichannel ALOHA," *IEEE Journal on Selected Areas in Communications*, vol. 35, no. 12, pp. 2736–2743, Dec 2017.

[13] M. Elkourdi, A. Mazin, and R. D. Gitlin, "Slotted Aloha-NOMA with MIMO beamforming for massive M2M communication in IoT networks," in *2018 IEEE 88th Vehicular Technology Conference (VTC Fall)*, August 2018, pp. 1–5.

[14] S. M. Kay, *Fundamentals of Statistical Signal Processing: Practical Algorithm Development*. Prentice Hall, 2013.